PRODUCTION ENGINEERING ARCHIVES 2025, 31(4), 493-503

PRODUCTION ENGINEERING ARCHIVES

ISSN 2353-5156 (print)
ISSN 2353-7779 (online)

Exist since 4th quarter 2013
Available online at https://pea-journal.eu

Optimized thermal regime modeling and experimental validation of electric heating in winter concreting

Baitak Apshikur[1], Anatoly Goltsev[1], Valeriy Chernavin[1], Murat Alimkulov[2], Ayazhan Aitkazina[1], Zhanar Rakizhanova[1]

[1] D. Serikbayev East-Kazakhstan Technical University, 19, Serikbayeva street, Ust-Kamenogorsk, Republic of Kazakhstan; bapshikur@edu.ektu.kz (BA); agoltsev-vko@edu.ektu.kz (AG); VChernavin58@mail.ru (VCh); AAytkazina@edu.ektu.kz (AA); ZhRakizhanova@ektu.кz (RZh)
[2] Mukhametzhan Tynyshpayev ALT University, 97, Shevchenko street, Almaty, Republic of Kazakhstan; alimkulov_murat@mail.ru
*Correspondence: bapshikur@edu.ektu.kz

Article history
Received 06.07.2025
Accepted 21.10.2025
Available online 12.12.2025

Keywords
winter concreting,
electric heating of concrete,
thermal modeling,
concrete strength development,
SHWPI heating wire technology.

Abstract
This paper investigates the thermal performance and early-age strength development of concrete cured using embedded electric heating wires (SHWPI – steel heating wire with polyethylene insulation) under winter conditions. A full-scale monolithic reinforced concrete slab was divided into four thermal zones for real-time monitoring using temperature sensors and ultrasonic testing over a 72-hour period. Experimental results were compared with thermal simulations conducted using the ELCUT software (WinConcrete module). The central zone reached a peak temperature of 35.6°C and achieved over 60% of the design strength within 48 hours, while edge zones attained only 52–56%. Actual temperature values were on average 12% lower than predicted, and strength deviations ranged from 8% to 13%. Based on this discrepancy, a correction factor of 0.08–0.13 is proposed to improve strength forecasting accuracy. The study highlights the critical role of temperature uniformity during the curing phase and demonstrates the value of integrating numerical modeling with real-time field monitoring. The findings are particularly relevant for optimizing electric curing strategies in cold climates, especially in regions with severe winters such as East Kazakhstan.

DOI: 10.30657/pea.2025.31.46

1. Introduction

Winter concreting presents significant technological and environmental challenges in cold regions such as East Kazakhstan, where temperatures can fall to −20°C or even −40°C. While concrete placement during warm seasons poses minimal difficulty, extreme winter conditions severely hinder the curing process, demanding additional thermal treatment to ensure early-age strength development. Delaying construction until spring is often economically unfeasible, particularly in rapidly developing urban areas.

Another critical challenge is posed by regional hydrological conditions. During spring and autumn floods, groundwater levels rise significantly – particularly along the banks of the Irtysh River (Muter et al., 2024). Consequently, meltwater and subsurface moisture can remain in prolonged contact with the lower sections of concrete structures. If concrete has not been adequately cured during winter, such saturated conditions can accelerate deterioration, especially in foundations and other exposed structural elements.

These challenges underscore the need for region-specific technological solutions that combine thermal treatment methods with predictive modeling of structural durability. Prior research has demonstrated the effectiveness of data-driven simulation tools in optimizing concrete performance under thermal stress in industrial settings (Alimkulov et al., 2025). Other studies have addressed flood risk mapping and the development of protective infrastructure to reduce hydrological impacts during seasonal transitions (Kurmangaliyev et al., 2023). Furthermore, integrated GIS-based transport models have highlighted the value of system-level planning in complex urban and environmental conditions – particularly in regions where high traffic loads and thermal fluctuations intensify cracking and deterioration in inadequately cured concrete structures such as bridges and load-bearing elements (Abedzhanova et al., 2023).

Building on these regional insights, this study investigates temperature distribution and strength development in winter-cast concrete using embedded electric heating.

Modern methods of winter concreting increasingly utilize self-heating concrete technologies based on electrically conductive additives, including steel fibers, graphite, carbon nanotubes (CNTs), and carbon black (Chang, et al., 2009; Liu et al., 2022). These methods enable improved temperature field uniformity and reduced energy consumption due to distributed internal heat generation.

In contrast, SHWPI (Steel Heating Wire with Polyethylene Insulation) systems, though widely used in post-Soviet countries, rely on embedded resistive wires and offer limited adaptability to complex geometries. Despite their simplicity, they often suffer from non-uniform heat distribution (Wang et al., 2020).

Comparative studies (Zhang et al., 2021) show that self-heating concrete mixtures can achieve more consistent early-age strength with lower energy input. However, such technologies often require advanced material processing and are cost-prohibitive for large-scale civil applications in harsh climates like East Kazakhstan.

Therefore, SHWPI systems remain relevant in regions where high-performance alternatives are not economically feasible. This study bridges this gap by combining traditional SHWPI with simulation-based optimization, thereby enhancing performance and ensuring local feasibility.

The objective is to improve construction quality under the extreme conditions of continental climates.

The scientific novelty of this study lies in the integration of experimental field monitoring with numerical thermal modeling using the ELCUT software suite to validate curing performance under real winter concreting conditions. Furthermore, the introduction of a correction factor (0.08–0.13) to account for deviations between predicted and actual early-age strength enhances the accuracy of strength forecasting in SHWPI-based systems – a methodology not widely applied in extreme continental climates.

Winter concreting techniques are generally classified into three categories: non-heating methods, combined methods, and heating-based approaches, which include both low- and high-temperature regimes (Zhuravlyov, 2020). In cold climates, the application of steel heating wires with vinyl insulation – known as SHWPI (Steel Heating Wire with Polyethylene Insulation) – embedded directly into the concrete mix enables more efficient heat distribution during the curing process (Yudina et al., 2017). This technology relies on steel conductors due to their high electrical resistance, making them suitable for controlled thermal treatment.

However, a key challenge remains in accurately determining the electrical heating parameters required for effective curing. Critical aspects – such as achieving uniform heat distribution, selecting appropriate thermal regimes, defining SHWPI wire characteristics, and optimizing wire spacing – are still insufficiently explored in the literature. Moreover, current recommendations for SHWPI selection often lack empirical validation.

Analysis of current winter concreting practices (Gnyrya et al., 2021) indicates that electric heating is often implemented without prior engineering calculations, relying instead on convenience or experience with similar structural components. In reality, thermal treatment regimes must be tailored to site-specific factors such as local climate, structural thickness, power availability, and the characteristics of materials and equipment used. Typically, these regimes are based on theoretical estimates of required thermal energy and electrical power consumption (Zhangabay et al., 2025).

Contemporary approaches enable the use of advanced software tools to model thermophysical processes and validate empirical formulas. However, a major limitation in current winter concreting practice with SHWPI systems is the insufficient application of computational modeling during the heating phase (Rakhimova et al., 2024).

Several researchers (Dudin et al., 2015; Korobkov et al., 2020) have highlighted the potential of using ELCUT and its WinConcrete module to simulate thermal treatment regimes in monolithic reinforced concrete structures. Their findings demonstrate the feasibility of modeling the heating process for large-scale elements such as structural beams.

In practical construction environments, temperature monitoring requires continuous measurement and meticulous documentation. For instance, concreting a 600 m² roof slab may involve as many as 100 temperature monitoring points (Utepov et al., 2022). This presents a logistical and technical challenge for personnel managing the SHWPI-based electric heating process. To ensure high-quality monolithic structures, thermal treatment parameters must be pre-calculated. In addition, factors such as the selected concreting method, electrical load on heating equipment and transformers, total power consumption, and internal temperature fields must be modeled, with appropriate algorithms developed accordingly. Such predictive modeling enables the early identification of underheated or overheated zones at the design stage (Zhang et al., 2023).

There is no universal solution suitable for all winter concreting scenarios; each method is effective only when applied correctly within its specific context. In practice, attention is often limited to calculating the total heating power, while important factors – such as the extended setting time of antifreeze-modified concrete mixes (typically 60–90 days at low temperatures) – are frequently underestimated (Reddy et al., 2019). Additionally, regulatory limitations on the use of antifreeze additives and heating methods are often overlooked.

The optimal ambient temperature for concrete hydration ranges from +15°C to +20°C. Nevertheless, construction activities in East Kazakhstan proceed throughout the year, even when ambient temperatures drop below freezing. In sub-zero conditions, unreacted water within the concrete mix freezes, interrupting the hydration process and hindering the formation of a solid cementitious matrix.

During this phase, internal stresses within the concrete increase significantly due to the 6–9% volumetric expansion that occurs when water freezes into ice. This process disrupts the developing crystal lattice, which cannot be fully restored even after temperatures rise above +5°C. While hydration may resume, it does so at a substantially reduced rate (Moldamuratov et al., 2024).

Upon thawing, free water creates thin films around inert particles, which impairs the formation of inter-particle bonds. As a result, the integrity of the concrete's monolithic structure is compromised. Even in the absence of complete failure, the compressive strength may not meet design specifications. This limit is referred to as the critical strength. If the concrete reaches this threshold prior to freezing, it can still achieve its design strength within 28 days under standard curing conditions (Tolentino et al., 2002; Buttignol et al., 2021).

The required level of critical strength varies depending on the concrete grade, structural function, and environmental exposure. In applications subjected to cyclic freeze–thaw conditions, hydraulic loads, or strict permeability requirements, the critical strength may need to reach up to 100% of the design value.

The post-placement cooling rate of concrete is primarily influenced by the structure's mass and is quantified using the surface modulus – the ratio of the structure's total surface area (m^2) to its volume (m^3).

East Kazakhstan is located within a sharply continental climate zone (approximately 47°–51° N, 80°–90° E), where winter temperatures frequently drop to −30°C or even −40°C. Such extreme conditions pose significant risks to concrete curing and compromise the overall quality of construction. As a result, optimizing the thermal treatment process presents a critical challenge for both engineers and researchers.

To address these challenges, the study applies advanced engineering tools – specifically ELCUT and its WinConcrete module – to simulate and optimize heat distribution under realistic construction conditions. The approach focuses on enhancing the performance of SHWPI-based electric heating systems in cold climates through precise layout configuration and thermal regime control (Mestnikov et al., 2018).

2. Materials and heating methodology for simulation of winter concreting

A variety of construction materials were selected for the simulation to replicate realistic thermal regimes and ensure effective heat retention during winter concreting. Galvanized C-25 profiled steel sheeting was used as a formwork base, featuring a thermal conductivity of 237 W/(m·K), specific heat capacity of 903 J/(kg·K), and density of 2700 kg/m³. Reinforcement bars were also incorporated, with a thermal conductivity of 58 W/(m·K) and specific heat capacity of 470 J/(kg·K).

The main structural material used in the simulation was class B30 concrete, which has a thermal conductivity of 2.07 W/(m·K), specific heat capacity of 1050 J/(kg·K), and density of 2500 kg/m³.

The concrete mixture used in this study was based on Class B30 with the following composition:

- Water-to-cement ratio (w/c): 0.45;
- Cement type: CEM I 42.5 N, Portland cement, 350 kg/m³.
- Aggregates:
- Fine aggregate (sand): 600 kg/m³;
- Coarse aggregate (gravel, 5–20 mm): 1200 kg/m³;
- Admixtures: Calcium nitrate-based antifreeze additive (3.5% by cement weight).

The SHWPI cable used was manufactured by *NII Energostal (Russia)*, with the following specifications:

- Heat output: 35 W/m;
- Insulation type: Polyethylene, double-layer;
- Cable voltage: 220 V;
- Diameter: 5.8 mm;
- Spacing between wires: 120 mm.

Reinforcement was provided by steel bars of 10 mm diameter, spaced at 150 mm intervals in both directions.

For strength monitoring, ultrasonic pulse velocity (UPV) testing was used with a Pundit PL-200 device.

Measurement points were spaced 250 mm apart along the slab, positioned 50 mm away from the heating wires and reinforcement intersections.

The concrete surface was smoothed and moistened to ensure consistent coupling between probe and surface.

For thermal insulation, 100 mm-thick extruded polystyrene foam of the *Penoplex* brand was used. This material has a thermal conductivity of 0.032 W/(m·K), specific heat capacity of 1320 J/(kg·K), and density of 40 kg/m³.

In addition, convective heating was implemented using SHWPI (Steel Heating Wire with Polyethylene Insulation), which was embedded directly into the concrete structure. The wire delivers a heat output of 35 W per linear meter and has a heat transfer coefficient of 9.5 W/(m²·K).

These materials were selected to establish optimal thermal conditions for maintaining stable internal temperatures during winter concreting and to ensure that the required structural strength is achieved under severe climatic conditions.

In current construction practice, methods for executing concrete and reinforced concrete works during winter are often chosen unilaterally, primarily based on the accumulated experience of the construction company. However, in many cases, these methods are not supported by rigorous engineering calculations or scientific validation. This can negatively impact the efficiency, safety, and overall quality of the final structure (Buttignol et al., 2021).

The technical decision-making process for selecting an appropriate winter concreting method should involve the following key steps:

- Performing thermal engineering calculations to justify the selected method;
- Selecting a concreting strategy that guarantees the required design strength of the concrete mix within the designated curing period under sub-zero temperatures;
- Designing the electrical supply network for heating elements and transformers;
- Estimating the total electrical capacity required, accounting for heat loss from structural surfaces and ambient temperature (when heating is applied);

- Modeling and analyzing the internal temperature field to identify zones that may be over- or underheated during the design phase.

It is important to emphasize that no single method is universally applicable to all winter concreting scenarios. Each technique is effective only when appropriately adapted to the specific engineering context. In this regard, combined thermal treatment methods – which incorporate multiple conventional approaches – provide the flexibility needed to perform concreting operations across a broad spectrum of climatic conditions. These methods also reduce reliance on strict temperature thresholds and allow for earlier formwork removal.

Overall, combined thermal treatment methods offer a reliable and high-quality solution for constructing monolithic concrete and reinforced concrete structures under winter conditions. Their versatility makes them suitable for both civil and industrial applications, particularly in regions with harsh climates (Zhangabay et al., 2025).

A comparative summary of various winter concreting methods and their effectiveness is presented in Table 1, where the methods are arranged in descending order of performance priority.

Table 1. Comparative analysis of methods and techniques for winter concreting of monolithic reinforced concrete structures.

No	Method	Preheating cycle (h)	Temperature rise cycle (h)	Isothermal holding cycle (h)	Cooling cycle (h)	Total treatment time (h)	Method ranking
1	Thermoactive formwork	–	$\frac{5-6}{4-5}$	$\frac{5-6}{4-5}$	$\frac{2-3}{2-3}$	$\frac{12-15}{10-13}$	1
2	Heating wire with insulation	–	$\frac{6-7}{5-5}$	$\frac{10-12}{6-8}$	-	$\frac{18-20}{12-155}$	2
3	Synergetic concreting	10–15	–	$\frac{8-16}{10-12}$	$\frac{6-8}{8-10}$	$\frac{20-24}{18-22}$	3
4	Preheating in bunkers followed by thermal insulation	15–20	–	–	$\frac{30-40}{24-30}$	$\frac{30-40}{24-30}$	4
5	Convective heating in tunnel formwork	–	24	46	13	70-80	5
6	Rod-type electric heating of structures	–	8–10	20–24	6–8	40–42	6
7	Plastic electric heating of structures	–	12–19	20–25	6–8	40–45	7
8	Heating in tents using electric radiators (for ambient t ≥ –10...–15°C)	–	10–12	8–28	8–10	50	8
9	Concreting with chemical additives (at t ≥ –10...–15°C)	–	–	–	–	14–40 days	9

3. Estimation of heat output for SHWPI heating systems

The findings of this study support the use of electric heating with SHWPI wires for winter concreting of thin-walled and medium-mass concrete structures. In this method, antifreeze additives are introduced into the concrete mix, and the surface is insulated with additional thermal protection materials. Heat is generated by electrical current passing through high-resistance steel conductors embedded within the concrete, functioning as heating elements (Gnyrya et al., 2021).

Antifreeze additives improve the workability of the concrete mix, facilitate its placement into formwork, and help prevent freezing during the critical early hours of the heating phase (Reddy et al., 2019). In winter concreting practice, SHWPI wires – experimentally tested in this study – consist of a steel conductive core and are embedded within the concrete prior to pouring. The typical heat output ranges from 35–40 W/m for reinforced concrete and 30–35 W/m for non-reinforced concrete.

One of the key factors influencing the efficiency of electric heating in concrete is the spacing (pitch) between SHWPI wire segments. In practical applications, spacing typically ranges from 50 mm to 200 mm. If the spacing is too wide, heat distribution becomes uneven; if it is too narrow, the concrete mix may overheat or even boil. Experimental observations also indicate that the minimum allowable distance between conductors and the bending radius is limited by the diameter of the wire cross-section (Alimkulov et al., 2025).

According to the national methodological guideline MDS 12-48.2009 of the Republic of Kazakhstan, titled *"Winter Concreting Using Heating Wires"*, the overall thermal transmittance coefficient KKK for a multilayer formwork system is calculated using the following formula:

$$K = \frac{1}{\frac{1}{\alpha_\lambda} + \sum_{i=1}^{i=n} \frac{\delta_i}{\lambda_i} + \frac{1}{\alpha_k}} \quad (1)$$

Where:

α_λ -is the external heat transfer coefficient from the environment to the outer surface of the formwork (W/m²·K);

δ_i- is the thickness of the *i*-th insulating layer (m);

λ_i -is the thermal conductivity of the *i*-th layer (W/m·K);

α_k -is the internal heat transfer coefficient from the formwork to the concrete surface (W/m²·K).

As outlined in the technical construction standard TSN 12-336-2007, *"Manufacturing of Structures Under Winter*

Concreting Conditions", the temperature difference between the surface of the heating wire and the surrounding concrete mix should not exceed 10°C. The temperature at the interface must be regulated to avoid boiling of the mix. This standard serves as the basis for selecting appropriate thermal regimes and wire specifications.

Additionally, under simplified conditions, the heat transfer coefficient KKK of the formwork system can be estimated using the following formula:

$$K = \frac{1}{\frac{1}{\alpha_\lambda} + \Sigma_{i=1}^{i=n} \frac{\delta_i}{\lambda_i}} \quad (2)$$

Where:

α_λ- is the heat release coefficient from the formwork system (W/m²·K);

δ_i -is the thickness (m) of the *i*-th insulating material layer;

λ_i-is the thermal conductivity (W/m·K) of the *i*-th insulation layer.

The primary objective of the thermal analysis is to determine the optimal spacing of SHWPI heating wires, as well as to establish the maximum temperature and the required duration of the heating process. The necessary heating power (in Watts) is defined using standardized nomograms, which consider the following parameters:

- the planar (surface) modulus of the structure,
- the target temperature differential between the concrete and the ambient environment,
- the heat transfer coefficient of the formwork, and
- the cement consumption rate (Mohapoo et al., 2025).

In accordance with the national construction guideline MDS 12-48.2009, the nomogram used to calculate the required heating power is presented in Figure 1.

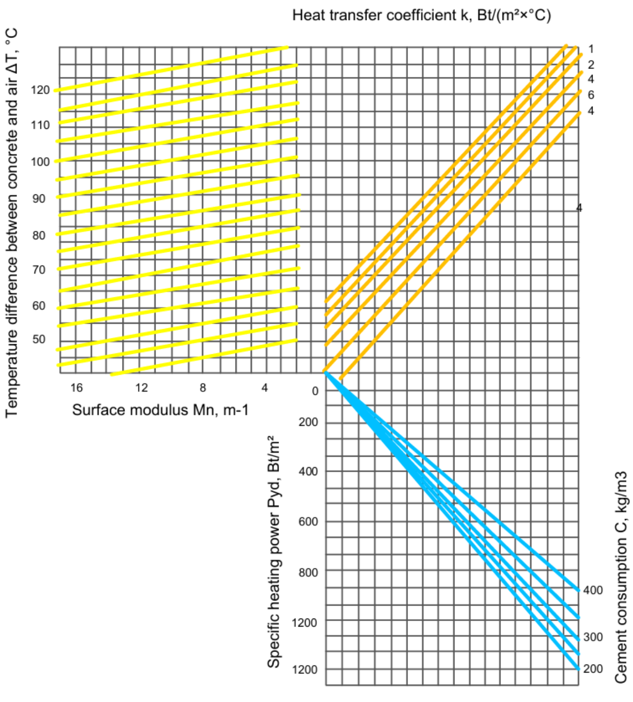

Fig.1. Nomogram for estimating heating power during winter concreting with SHWPI wires

4. Finite element modeling of the concrete heating process

Modern computational software packages enable the effective determination and assignment of concrete heating parameters (Mohapoo et al., 2025; Korobkov et al., 2020; Mestnikov et al., 2018). In this study, thermal modeling was conducted in cooperation with the engineering team at "LegionStroyGrad" LLP. The simulations were performed using the ELCUT software package, which is based on the finite element method (FEM) and is widely used for solving complex engineering and thermophysical problems.

ELCUT includes a specialized WinConcrete module that allows for the calculation of temperature fields within concrete, the analysis of their distribution across thickness, the identification of temperature variations at joint points, the construction of strength gain graphs, and the assessment of thermal deformations resulting from heating with SHWPI wire (Dudin et al., 2015).

As part of the study, the heating process of the technical floor slab of a commercial building located at 10 Pobedy Avenue was analyzed using computer modeling. The slab was laid over galvanized profiled sheeting installed on steel beams. The slab structure connects to monolithic reinforced concrete columns. The maximum thickness of the slab layer was 90 mm (Figure 2).

Fig. 2. Monolithic floor slab of Block B at elevation −0.050 m

The monolithic slab was cast under subzero ambient temperature conditions (−10 to −15°C). The heating process was carried out using SHWPI wire, which was embedded into the slab at 100 mm intervals, as shown in Figure 3.

The upper surface of the monolithic slab at elevation −0.050 m was insulated with 100 mm-thick Penoplex-brand extruded polystyrene foam. Heat loss primarily occurred through the monolithic columns located along the perimeter of the slab, as well as through the galvanized profiled sheeting at the bottom of the structure.

The cross-sectional layout of the slab used for thermal analysis in the ELCUT software package is presented in Figure 4.

Fig. 3. General view of the installed SHWPI wire and transformer

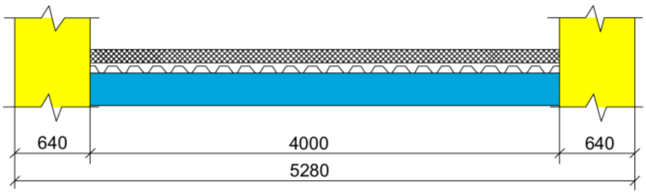

Fig. 4. Cross-section of the analyzed slab between beams

A computational model was developed in the ELCUT software package using the finite element method (Doudkin et al., 2019a). This model accounted for the design geometrical dimensions as well as the physical and mechanical properties of the materials used (Doudkin et al., 2019b).

The modeled configuration represented a half-section of the slab located between two steel beams, and the computational domain was divided into two symmetrical parts. The finite element mesh for the designed slab model is presented in Figure 5.

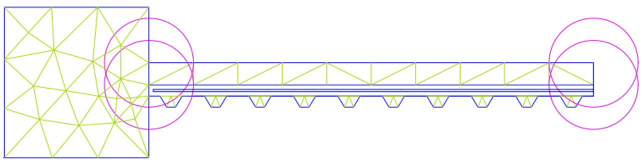

Fig.5. Finite element mesh of the computational slab model

The thermodynamic characteristics and physical parameters of the materials used in the simulation are presented in Table 2. The initial conditions adopted for the thermal simulation are summarized in Table 3. The heat output density is a variable parameter, while the radiation and heat dissipation coefficients are automatically calculated within the WinConcrete add-on module, depending on temperature and time parameters (Korobkov et al., 2020).

Table 2. Physical and thermophysical properties of the materials used

Material name	Density, ρ (kg/m³)	Thermal conductivity, λ (W/m·K)	Specific heat capacity, c (J/kg·K)	Characteristics and applications
alvanized profile sheet C-25	2700	237	903	Used in the lower part of the formwork
Reinforcement	-	58	470	Used as reinforcement in reinforced concrete
Concrete B30	2500	2.07	1050	Main structural material
Polystyrene foam "Penoplex"	40	0.032	1320	Thermal insulation for the upper surface (100 mm thickness)
SHWPI wire (steel heating wire)	-	-	-	Heating element, power output: 35 W/m (reinforced); 30–35 W/m (non-reinforced)

Table 3. Initial conditions adopted for the thermal simulation

Parameter	Value
Ambient temperature	–10°C
Concrete mix temperature	+10°C
Reinforcement temperature	–5°C
Slab surface temperature	+10°C (under convective heating)
Convective heat transfer coefficient	9.5 W/m²·K
SHWPI wire heat output	35 W/m (equivalent to 0.0046 °C/s)
Slab materials	Concrete B30, profiled steel, rebar
Thermal insulation	Polystyrene foam "Penoplex", 100 mm

5. Results and Discussion

The SHWPI heating wires were incorporated into the model as discrete vertices with specified heat output capacities. Following the input of all necessary parameters, an initial thermal field was generated to represent the temperature distribution within the concrete structure at the time of placement, i.e., prior to the start of the heating process.

The program's reference database includes a wide range of values for the specific heat capacity, thermal conductivity, and density of various construction materials.

The resulting initial temperature distribution in the slab is shown in Figure 6**.**

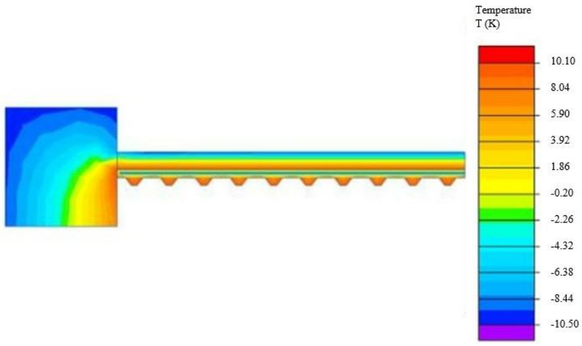

Fig.6. Temperature distribution in the slab before the start of heating

It is important to note that if the concrete mix is overheated during preparation or early curing, accelerated evaporation of mixing water may occur. This disrupts the water-cement ratio and reduces the final compressive strength of the concrete. The risk of early microcrack formation increases especially under sharp thermal gradients, as reported in previous studies on concrete durability in cold climates.

In the framework of this study, the computational time step was set to 2 hours. The target duration for maintaining stable temperature conditions and the cooling phase of the concrete structure was defined as 24 hours, with the total heating period set to 48 hours.

The simulation process was initiated with a preliminary (approximate) calculation, referred to as a "first-pass" analysis. The software suite performs the simulation by accounting for the specific heat capacity and thermal conductivity of all structural materials, along with convective heat exchange with the surrounding environment and convective heating from the underside of the structure.

After the initial 2 hours of heating, localized heat accumulation zones and areas of heat loss – particularly at the junctions with the supporting columns – became apparent. The results corresponding to this stage of the simulation are presented in Figure 7.

As observed from the thermal field distributions, no freezing of the concrete mix occurred during the first two hours. The top surface of the slab structure was insulated with thermal protection material, while the ribbed surface of the galvanized profile sheet on the underside was heated to prevent cooling of the concrete from below.

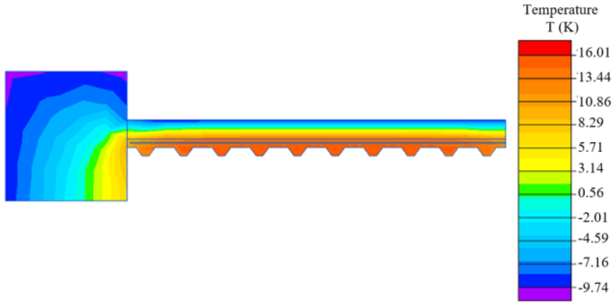

Fig.7. Temperature distribution in the slab after two hours of heating

In addition, it can be concluded that the heating process was not uniform. The areas in direct contact with the SHWPI wire heated up more quickly, whereas lower temperatures were observed in zones of heat loss. The generated graphs illustrate the distribution of heat within the concrete, enabling the identification of critical heat loss points and providing a basis for adjusting the heating parameters accordingly (Gnyrya et al., 2021).

The final results of the preliminary simulation (first-pass analysis) after 48 hours of heating are presented in Figure 8, where the location of the SHWPI heating wires can be identified based on the zones of elevated temperature. This simulation represents a preliminary (first-pass) calculation and does not account for the exothermic effects of the hydration reaction. By enabling the WinConcrete add-on module, the simulation can be refined to obtain detailed temperature distribution graphs as well as the concrete strength gain curve.

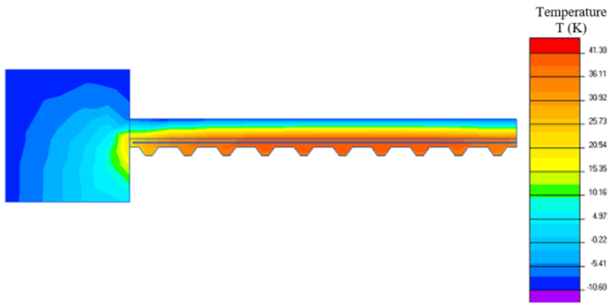

Fig. 8. Temperature distribution in the slab after 48 hours of heating

According to the given model, the concrete was heated up to a temperature of 44°C, resulting in a temperature difference of approximately 54°C relative to the ambient environment. The software allows the user to determine the optimal moment to remove the thermal insulation layer and to evaluate the evolution of mechanical strength after the electric heating is turned off (Farzana et al., 2023).

The thermal resistance values of the slab structure are maintained by reducing the temperature of the concrete mix (t_conc) and removing the insulation layer 24 hours after the heating process ends. At that stage, the concrete attains approximately 75% of its design strength (based on the standard 28-day curing period).

The amount of heat released is directly proportional to the quantity of binder (cement) in the mix. The software divides the slab into equal segments, allowing the operator to track compressive strength development at various times and locations throughout the structure.

The slab structure was divided into three thermal blocks, numbered sequentially:

- Blocks No. 1 and No. 3 correspond to areas adjacent to the columns;
- Block No. 2 represents the central portion of the slab.
- Block No. 4 was designated as an output block for calculating average thermal and mechanical properties across the entire structure.

The simulation results are presented in infographic form. Figure 9 illustrates the temperature dynamics of the concrete blocks over 72 hours.

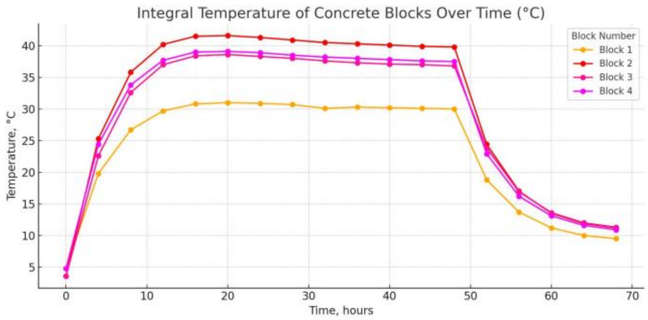

Fig. 9. Temperature-time graph of the concrete slab blocks

As seen in the graph, the concrete temperature increased rapidly during the first 20 hours and then stabilized. For example, in Block No. 2, the temperature peaked at approximately 42°C around the 20th hour and remained near this level until hour 48. In Block No. 1, the peak temperature was lower-around 31°C.

After 48 hours, the temperature began to gradually decrease across all blocks. By the end of the 72 hours, the temperature stabilized between 9°C and 11°C.

This temperature behavior reflects the real-time dynamics of internal hydration reactions and heat exchange processes within the concrete mix.

According to the collected data, an increase in temperature was correlated with an increase in compressive strength. Specifically, in areas where the temperature exceeded 35°C, the compressive strength reached more than 70%, while in zones where the temperature remained below 25°C, the strength development was significantly lower.

This demonstrates that by controlling the temperature regime of the concrete mix, one can directly influence the mechanical performance of the material.

Figure 10 presents the temperature-based strength gain graph of concrete in different zones, expressed as a percentage. The graphs illustrate the rate of concrete strength gain across various zones. Figure 10, which characterizes changes in concrete strength, demonstrates how strength development evolves as a function of both temperature exposure and time. In all blocks, the strength increases actively within the first 20 to 28 hours.

Blocks No. 2, 3, and 4 reach approximately 66–68% of the design strength after 72 hours.

Block No. 1 develops strength at a slower rate, reaching only about 57–58%.

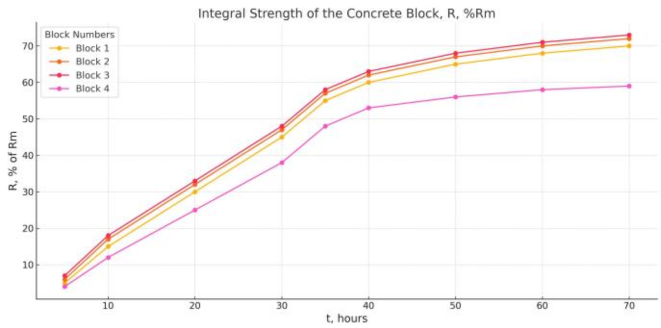

Fig. 10. Graph of concrete strength gradient over the heating period

Actual temperature values were on average 12% lower than predicted, and strength deviations ranged from 8% to 13%.

These deviations were systematically analyzed to evaluate the model's predictive accuracy. The central zone reached 35.6°C versus a predicted 40.2°C, while edge zones also showed lower strength values than expected.

A correction factor (CF) was proposed to account for this discrepancy. Table 4 summarizes the comparison.

Table 4. Comparison of simulated and measured compressive strength with corresponding correction factors

Zone	Simulated Strength (MPa)	Measured Strength (MPa)	Deviation (%)	Correction Factor
Center	23.5	21.8	7.2	0.08
Edge Left	21.7	18.9	12.9	0.13
Edge Right	22.1	19.6	11.3	0.11

These differences confirm the direct influence of the initial temperature regime on strength development. The higher the temperature, the more intense the cement hydration process within the concrete. This is especially critical in heat-treated concrete structures.

6. Correlation of modeled and measured strength parameters

As previously noted, the floor slab structure was conditionally divided into four temperature zones and segmented into a grid, with each section assigned an individual identification number. Zones No. 1 and No. 3 were located at the edges of the slab, Zone No. 2 was situated in the central part, and Zone No. 4 served as an integrated reference block for assessing the average values of temperature and strength.

The temperature of the hardening concrete and the associated strength characteristics were measured in real time using electronic thermometers and the UKS-MG4 ultrasonic device in accordance with GOST 17624–2012 (national standard).

The monitoring results for the thermal regime and concrete strength are presented in tabular form. Table 4 provides concrete temperature values for each thermal block at various stages of the thermal treatment process. Table 5 contains the ultrasonic strength measurements in megapascals (MPa). Additionally, Table 6 shows the strength gain as a percentage of the design (grade) strength, allowing the tracking of strength development over time. A comparative analysis of the three tables establishes a direct correlation between the intensity of heating and the strength development of concrete in each temperature block over various time intervals.

Table 5. Measured concrete temperatures during the heating process

Block number	Temperature distribution across slab zones over time, °C																		
	"Duration of the electric heating process, hours																		
a	0	4	8	12	16	20	24	28	32	36	40	44	48	52	56	60	64	68	72
1	3.0	15.3	21.0	23.5	24.4	24.5	24.4	24.3	23.8	23.9	23.9	23.8	23.7	14.5	10.3	8.3	7.3	6.9	6.6
2	2.2	21.3	30.5	34.4	35.6	35.6	35.4	35.0	34.7	34.5	34.3	34.1	34.1	20.5	14.0	10.9	9.5	8.9	8.5
3	2.0	17.0	24.9	28.4	29.5	29.6	29.4	29.2	28.8	28.6	28.4	28.4	28.2	17.9	12.5	9.9	8.6	8.1	7.7

Table 6. Ultrasonic device data on concrete strength over the heating duration

Block number	Concrete strength by ultrasonic method across slab zones, MPa																		
	Duration of the electric heating process, hours																		
a	0	4	8	12	16	20	24	28	32	36	40	44	48	52	56	60	64	68	72
1	0	0.89	2.47	4.26	5.98	7.5	8.9	7.3	11.3	12.2	13.1	13.9	14.7	15.2	15.5	15.7	15.9	16.1	16.2
2	0	1.05	3.24	5.74	8.05	10.0	11.7	13.1	14.3	15.3	16.3	17.1	17.8	18.3	18.6	18.7	18.9	19.0	19.1
3	0	0.90	2.75	4.92	6.99	8.8	10.3	11.6	12.8	13.8	14.6	15.4	16.1	16.6	16.9	17.1	17.2	17.4	17.5

Table 7. Concrete strength gain gradient during heating (% of nominal/design grade strength)

Block number	Ultrasonic concrete strength by slab zones, as a percentage of design strength																		
	Duration of the electric heating process, hours																		
a	0	4	8	12	16	20	24	28	32	36	40	44	48	52	56	60	64	68	72
1	0	2.85	7.91	13.62	19.14	24.1	28.6	23.4	36.1	39.2	42.0	44.6	47.0	48.6	49.6	50.3	50.9	51.4	52
2	0	3.37	10.37	18.38	25.75	32.1	37.4	41.9	45.9	49.1	52.1	54.7	57.1	58.6	59.4	60	60.4	60.8	61.2
3	0	2.87	8.79	15.75	22.36	28.1	33.1	37.2	40.9	44.1	46.9	49.4	51.7	53.2	54.1	54.7	55.2	55.7	56.0

Based on the data presented in Tables 4–6, a graphical correlation was developed between concrete temperature and strength gain across different thermal zones. Figure 10 illustrates this relationship, highlighting the dependence of strength development on internal heating conditions. The plot shows that concrete zones with higher average temperatures generally demonstrate faster and greater strength gain. For instance, in thermal zones where the temperature exceeds 30°C, the concrete achieves over 50% of its design strength, whereas zones with lower temperatures (around 20°C) show a slower gain, limited to approximately 45–46%. This indicates that uniform and sufficient heating significantly accelerates the hardening process. Thus, a direct relationship between internal concrete temperature and strength gain was identified in the analysis. Thermal zone 2 (central area) demonstrated both the highest temperatures and the most significant strength development, confirming the effectiveness of uniform and sufficient heating. In contrast, zones 1 and 3 (located along the slab edges) exhibited lower temperatures and correspondingly slower strength growth. These results validate the modeled heating process and highlight the importance of proper thermal management. They also provide a practical foundation for applying correction coefficients in future structural concreting under winter conditions.

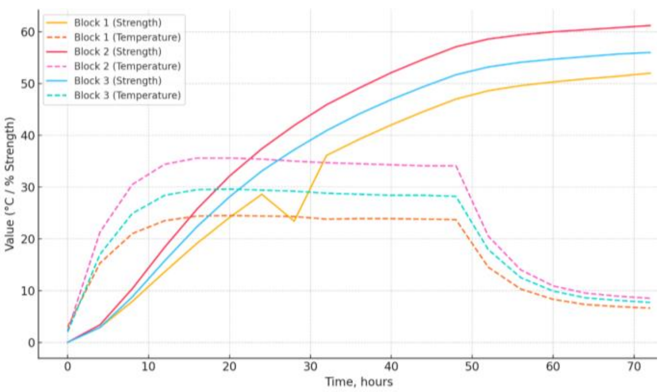

Fig. 11. Concrete temperature and strength gain over time

7. Summary and conclusion

As a result of the comprehensive experimental and modeling study, a clear and direct correlation between the internal thermal regime of the concrete and the rate of early-age strength gain was established. Experimental data showed that when internal temperatures exceeded 35°C, concrete achieved more than 60% of its design compressive strength within 48–72 hours. In contrast, areas where temperatures remained near 25°C reached no more than 52% of the expected strength. These findings reinforce the necessity of maintaining a uniform and adequately elevated curing temperature, particularly under winter concreting conditions.

The use of Steel Heating Wire with Polyethylene Insulation (SHWPI) for thermal treatment was analyzed in detail. The required heating power parameters were determined, and the procedures for temperature data collection, storage, and analysis during monolithic concreting were described. While the SHWPI technology itself is not novel and has been widely applied in cold-weather concreting for decades, this study contributes practical advancements by combining SHWPI with numerical simulation and correction mechanisms to improve predictive reliability.

A comparative analysis between measured field data and simulated outputs using the ELCUT software with the WinConcrete add-on revealed notable discrepancies. On average, the simulated temperature values were 12% higher than actual readings, typically differing by 0.3–0.5°C. Similarly, ultrasonic measurements of compressive strength revealed deviations of 8–13% from the theoretical model values. These differences were most pronounced near the slab edges, where boundary conditions reduced heating efficiency.

To address this, a correction factor ranging from 0.08 to 0.13 was introduced based on experimental calibration. Incorporating this factor into the modeling process significantly improves the accuracy of early-age strength predictions, especially when used in combination with ELCUT simulations. This adjustment also lays the groundwork for the future development of intelligent control algorithms, including machine-learning-based optimization of heating parameters.

Although SHWPI technology lacks novelty in principle, the proposed approach demonstrates scientific contribution by enhancing model reliability, reproducibility, and field applicability through data-driven correction. The methodology developed in this study can support engineers and construction planners in designing cost-effective and energy-efficient thermal regimes, particularly in remote or resource-limited cold climate regions.

In conclusion, the observed discrepancies between simulation and experimental results fall within acceptable engineering tolerances and validate the overall methodology. The proposed correction mechanism enhances the reliability of thermal modeling and ensures safer and more efficient concreting operations during severe winter conditions.

Conflicts of interest

The authors declare that they have no known financial or personal conflicts of interest that could influence the work reported in this paper. Furthermore, all listed authors have reviewed and approved the final version of the manuscript.

Reference

Abedzhanova, A., Dzhaxylykov, A., P. A. Rasskazov, B. Apshikur, and G. Islyam., 2023. Automated system for optimizing the movement of urban passenger transport using GIS. Int. Arch. Photogramm. Remote Sens. Spatial Inf. Sci., XLVIII-5/W2-2023, 1–8, DOI: 10.5194/isprs-archives-XLVIII-5-W2-2023-1-2023, 2023

Alimkulov, M., Apshikur, B., Goltsev, A., Chernavin, V., Chigambayev, T., Kunanbayev, A., 2025. Data-driven modeling and experimental validation of heat-resistant concrete for industrial furnace lining. Vibroengineering Procedia, vol. 58, pp. 354–360, May 2025, DOI: 10.21595/vp.2025.25013

Apshikur, B., Kurmangaliyev, T., Goltsev, A., Alimkulov, M., Kapasov, A., 2023. The method of multi-criteria analysis for determining the flood-hazardous area and the development of protective structures. Int. Arch. Photogramm. Remote Sens. Spatial Inf. Sci., XLVIII-5/W2-2023, 9–17, DOI: 10.5194/isprs-archives-XLVIII-5-W2-2023-9-2023, 2023

Buttignol, T.E.T., Bitencourt, L.A.G. 2021. A Transient Creep Investigation Applied to the Mesoscopic Analysis of Plain Concrete under Uniaxial Compression at High Temperature. Fire Safety Journal, Elsevier Ltd, 126, 103484. DOI: 10.1016/j.firesaf.2021.103484

Chang, Ch., Ho, M., Song, G., Mo, Y., Li, H., 2009. A feasibility study of self-heating concrete utilizing carbon nanofiber heating elements. Smart Materials and Structures. 18. 127001. DOI: 10.1088/0964-1726/18/12/127001

Dudin, M. Vatin, N., Barabanshchikov, Y., 2015. Modeling a set of concrete strength in the program ELCUT at warming of monolithic structures by wire. Magazine of Civil Engineering. 54. 33-45. DOI: 10.5862/MCE.54.4

Doudkin, M., Apshikur, B., Kim, A., Ipalakov, T., Asangaliev, E., Mlynczak, M., 2019a. Development of an installation for shear ground testing in the railway track construction. News of the National Academy of Sciences of the Republic of Kazakhstan, Series of Geology and Technical Sciences, 6(438), 22–35. DOI:10.32014/2019.2518-170X.152

Doudkin, M., Apshikur, B., Kim, A., Ipalakov, T., Asangaliev, E., Mlynczak, M., Tungushbayeva, Z., 2019b. Development of mathematical models describing the processes occurring in the railway track construction as a whole, or in the work of its individual elements. News of the National Academy of Sciences of the Republic of Kazakhstan, Series of Geology and Technical Sciences, 5(437), 6–15. DOI: 10.32014/2019.2518-170X.120

Farzana, M., Rajesh, Ch., Han-Jin, O., Doo-Yeol, Y., Ramita M., Jung, H., 2023. Design and performance evaluation of an electrically heated concrete panel for sustainable winter maintenance, Developments in the Built Environment, Volume 16, 2023, 100259, ISSN 2666-1659, DOI: 10.1016/j.dibe.2023.100259

Gnyrya, A., Korobkov, S., Gaag, I., 2021. Numerical solution of the thermal problem for electric heating of concrete structures in winter. E3S Web of Conferences, 258, 09048. DOI: 10.1051/e3sconf/202125809048

Korobkov, S., Mikhailov, D., Gnyrya, A., Titov, M., 2020. Modeling the hardening process of monolithic reinforced concrete structures in Elcut Pro software package. IOP Conference Series: Materials Science and Engineering. 953. 012030. DOI:10.1088/1757-899X/953/1/012030

Liu, J., Sun, C., Zhang, R., Wang, L. 2022. Thermal and electrical properties of carbon-nanotube modified concrete under low-temperature conditions, Journal of Materials in Civil Engineering, 34(9), 04022254. DOI: 10.1061/(ASCE)MT.1943-5533.0004294

Mestnikov, A., Turantaev, G., Fedorov, V., 2018. Mathematical modeling of temperature fields and concrete strength during winter concreting of building structures. MATEC Web of Conferences. 245. 03009. DOI:10.1051/matecconf/201824503009

Mohapoo, R., Chakraborty, R., Yeon, J., 2025. Development of an Electrically Heated Sidewalk System for Enhanced Winter Pedestrian Safety. Buildings. 15. 533. DOI: 10.3390/buildings15040533

Moldamuratov, Zh., Ismailova, A., Tukhtamisheva, A., Yeskermessov Zh., Rakhimov, Murat., 2024. Experimental study of asphalt concrete as the optimal material for lining irrigation canals. Nanotechnologies in Construction A Scientific Internet-Journal, 16, 125-139. DOI: 10.15828/2075-8545-2024-16-2-125-139

Muter, O., Gudra, D., Daumova, G., Idrisheva, Zh., Rakhymberdina, M., Tabors, G., Dirnena, B., Dobkeviča, L., Petrova, O., Apshikur, B., Luņģe, M., Fridmanis, D., Denissov, I., Bekishev, Y., Kasparinskis, R., Mukulysova, Z., & Polezhayev, S., 2024. Impact of Anthropogenic Activities on Microbial Community Structure in Riverbed Sediments of East Kazakhstan. Microorganisms, 12, 246. DOI: 10.3390/microorganisms12020246

Rakhimova, G., Zhangabay, N., Samoilova, T., Rakhimov, M., Kropachev, P., Stanevich, V., Karacasu, M., Ibraimova, U., 2024. Computational Research of the Efficiency of Using a Three-Layer Panel Made of Highly Porous Polystyrene Concrete. Materials, 17, 4133. DOI: 10.3390/ma17164133

Reddy, P., Narasimha, N., Javed A., 2019. Effect of Antifreeze Admixtures on Cold Weather Concrete. International Journal of Engineering. 32. 366-372. DOI: 10.5829/ije.2019.32.03c.03

Tolentino, E., Lameiras, F. S., Gomes, A. da, S., Vasconcelos, W., 2002. Structural Evaluation and Performance of Portland Cement Concretes After Exposure to High Temperatures. Materials Research. 5. DOI: 10.1590/S1516-14392002000100005

Utepov, Y., Tulebekova, A., Aldungarova, A., Zharassov, Sh., Sabitov, Y., 2022. Performance of a wireless sensor adopted in monitoring of concrete strength. International Journal of GEOMATE, 23, 73-80. DOI: 10.21660/2022.95.3265

Yudina, A., Oganyan, R., 2017. Technology of winter concreting of monolithic constructions with application of heating cable. Architecture and Engineering, 2, 43-48. DOI: 10.23968/2500-0055-2017-2-2-43-48

Zhang, Y., Sun, H., Qian, X., Wang, J., Tan, G., 2023. Research on the Electrosensitivity and Electrothermal Properties of Intelligent High-Performance Concrete Materials. Materials. 17. 54. DOI: 10.3390/ma17010054

Zhang, D., Yu, K., Xu, Y., Li, Q., Wang, K., 2021. Electrically conductive and self-heating cementitious composites: A review on mechanisms, materials, and future development. Cement and Concrete Composites**,** 118, 103985. DOI: 10.1016/j.cemconcomp.2021.103985

Zhangabay, N., Oner, A., Rakhimov, M., Tursunkululy, T., Abdikerova, U., 2025. Thermal Performance Evaluation of a Retrofitted Building with Adaptive Composite Energy-Saving Facade Systems. Energies, 18, 1402. DOI: 10.3390/en18061402

Zhuravlyov, E., 2020. Review and analysis of winter concreting methods, used on construction sites in Russia, IOP Conference Series, Materials Science and Engineering, 880, 012029. DOI: 10.1088/1757-899X/880/1/012029